JOURNAL OF SOLID STATE CHEMISTRY 114, 236–241 (1995)

Relationship between the Electrical Properties and Crystal Structure of $(La_{1-x}Nd_x)CrO_3$ $(0 \leq x \leq 1.0)$

Hideki Taguchi[1] and Mahiko Nagao

Research Laboratory for Surface Science, Faculty of Science, Okayama University, Okayama 700, Japan

and

Yasuo Takeda

Department of Chemistry, Faculty of Engineering, Mie University, Tsu 514, Japan

Received January 25, 1994; in revised form April 25, 1994; accepted April 27, 1994

Perovskite-type $(La_{1-x}Nd_x)CrO_3$ has the orthorhombic $GdFeO_3$-type structure with the space group *Pnma*. The electrical resistivity of $(La_{1-x}Nd_x)CrO_3$ $(0 \leq x \leq 1.0)$ was measured in the temperature range 300 to 1000 K. Although the cell volume decreases linearly with increasing x, significant compositional dependence on electrical resistivity is not found. $(La_{1-x}Nd_x)CrO_3$ is a p-type semiconductor with an activation energy of ca. 0.26 to ca. 0.28 eV. Rietveld analysis and XPS measurements indicate that each CrO_6 octahedron has little distortion and that the decrease in the angles for Cr–O(1)–Cr or Cr–O(2)–Cr is caused by the linear decrease in the cell volume.

INTRODUCTION

$LaCrO_3$ has an orthorhombic perovskite-type structure with $a = 5.479$ Å, $b = 7.756$ Å, and $c = 5.513$ Å (1). $LaCrO_3$ exhibits antiferromagnetism with a Néel temperature (T_N) of 282 K, and obeys the Curie–Weiss law with a Curie constant (C) of 2.41 (2). Rao *et al.* measured the electrical properties of rare earth *ortho*-chromites, *ortho*-manganites, and *ortho*-ferrites (3). According to their report, $LaCrO_3$ is a p-type semiconductor with an activation energy (E_a) of ca. 0.22 eV. Goodenough proposed the one-electron energy diagram for $LaCrO_3$ consisting of partially filled σ^* orbitals and π^* holes (4). The localized π^* orbitals of α and β spins at a given cation are split by the intra-atomic exchange (E_{ex}), and the collective σ^* orbitals are also split by E_{ex}.

$NdCrO_3$ also has an orthorhombic perovskite-type structure with $a = 5.430$ Å, $b = 7.692$ Å, and $c = 5.488$ Å (1). Because of the lanthanide contraction, the cell volume of $NdCrO_3$ is smaller than that of $LaCrO_3$. $NdCrO_3$ exhibits antiferromagnetism with $T_N = 224$ K, and does not obey the Curie–Weiss law (2). The difference in the magnetic properties of $LaCrO_3$ and $NdCrO_3$ is strongly influenced by the type of rare-earth ion and/or the Cr–O distance.

Cubic perovskite-type $SrFeO_{3-\delta}$ has an anion-deficient nonstoichiometry (5). The Fe–O distance decreases linearly with decreasing δ, and the electrical properties are strongly influenced by the Fe–O distance. From these results, it is important to estimate the overlap between cationic t_{2g} and anionic p_π orbitals. The electrical properties for $NdCrO_3$ have not been reported. Since the cell volume of $NdCrO_3$ is smaller than that of $LaCrO_3$, the overlap between the chromium t_{2g} and oxygen p_π orbitals of $NdCrO_3$ may vary from that of $LaCrO_3$, and the electrical conductivity for $NdCrO_3$ will be different from that of $LaCrO_3$.

In the present study, we synthesized perovskite-type $(La_{1-x}Nd_x)CrO_3$ $(0 \leq x \leq 1.0)$ to study the relationship between the Cr–O distance and the electrical properties. These results will provide information regarding the overlap between the chromium t_{2g} and oxygen p_π orbitals in orthorhombic perovskite-type oxide systems.

EXPERIMENTAL

$(La_{1-x}Nd_x)CrO_3$ $(0 \leq x \leq 1.0)$ samples were prepared by a standard ceramic technique. Dried La_2O_3, Nd_2O_3, and Cr_2O_3 powders (Nacalai Tesque, Japan) were weighed in the appropriate proportions and milled for a few hours with acetone. After the mixed powders were dried at 373 K, they were calcined at 1173 K for a few hours in air, then fired at 1623 K for 24 hr in air. In order to measure the electrical resistivities, the powders were pressed into a rod form under a pressure of 50 MPa, and the rod was sintered at 1623 K for 12 hr in air.

[1] To whom correspondence should be addressed.

0022-4596/95 $6.00

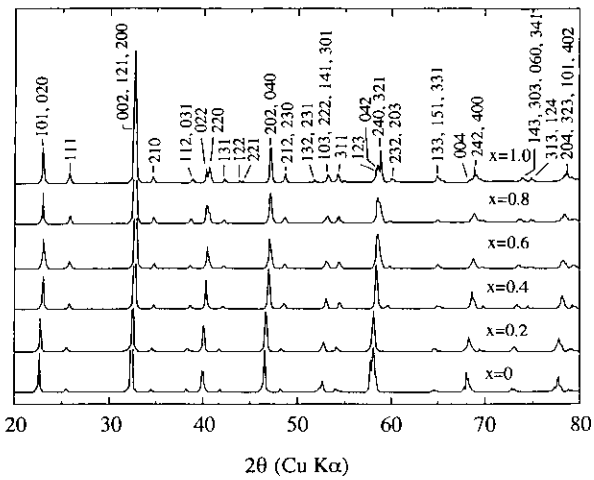

FIG. 1. X-ray powder diffraction patterns for the system $(La_{1-x}Nd_x)CrO_3$.

The phases of the samples were identified by X-ray powder diffraction (XRD) with monochromatic Cu$K\alpha$ radiation (RAD-1C, Rigaku, Japan). The cell constants of the samples were determined from high-angle reflections with Si as an external standard. The a-axis of Si is 5.4309 Å (6). The structure refinement was carried out by Rietveld analysis of the X-ray powder diffraction data with the "RIETAN" program written by Izumi (7). X-ray diffraction data were collected by step scanning over an angular range of $20° \leq 2\theta \leq 80°$ in increments of 0.02° (2θ) with monochromatic Cu$K\alpha$ radiation. The electrical resistivity of the samples was measured in air by a standard four-electrode technique in the temperature range 300–1000 K (195A, Keithley, USA and 7651, Yokogawa, Japan).

X-ray photoelectron spectroscopy (XPS) measurement of the samples was carried out for the La3d, Nd3d, Cr2p, and O1s levels of the samples using Mg$K\alpha$ radiation (ESCA-750, Shimadzu, Japan) at room temperature. The energy calibration was made against the C 1s level from a usual contamination.

RESULTS AND DISCUSSION

X-ray powder diffraction patterns of $(La_{1-x}Nd_x)CrO_3$ ($0 \leq x \leq 1.0$) were completely indexed as the orthorhombic perovskite-type ($GdFeO_3$-type) structure and are shown in Fig. 1. Figure 2 shows the relationship between the cell constants (a, b-, and c-axes) and the composition. With increasing x, the a-axis decreases slightly, has a minimum value at $x = 0.6$, then increases. On the other hand, both the b- and c-axes decrease monotonically with increasing x. Figure 3 shows the relationship between cell volume and composition. The cell volume of $LaCrO_3$ is 234.4 Å^3, and decreases linearly to 228.6 Å^3 ($x = 1.0$) with increasing x. The ionic radii of a La^{3+} ion and a Nd^{3+} ion with a coordination number (CN) of 12 are 1.35 and 1.27 Å, respectively (8, 9). The linear decrease in the cell volume is explained by the difference in the ionic radius between the La^{3+} and Nd^{3+} ions.

Figure 4 shows the relationship between the electrical resistivity (ρ) of $(La_{1-x}Nd_x)CrO_3$ and the reciprocal temperature. Although the cell volume decreases linearly with increasing x, as seen in Fig. 3, we could not find significant compositional dependence on the electrical resistivities. All samples were p-type semiconductors above room temperature. The relationship between log ρ and $1000/T$ was linear at high temperatures. We calculated an activation

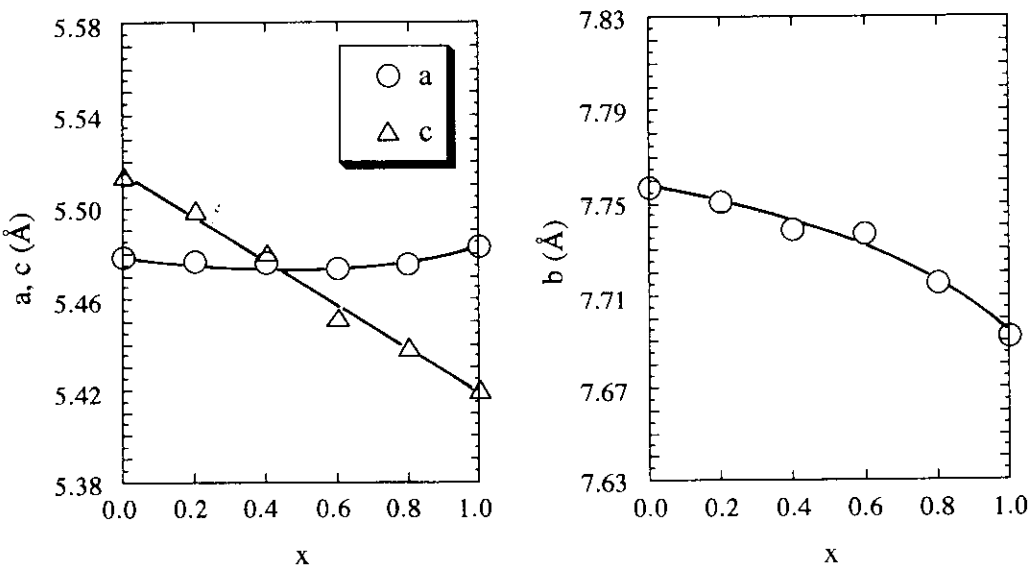

FIG. 2. Cell constants vs composition for the system $(La_{1-x}Nd_x)CrO_3$.

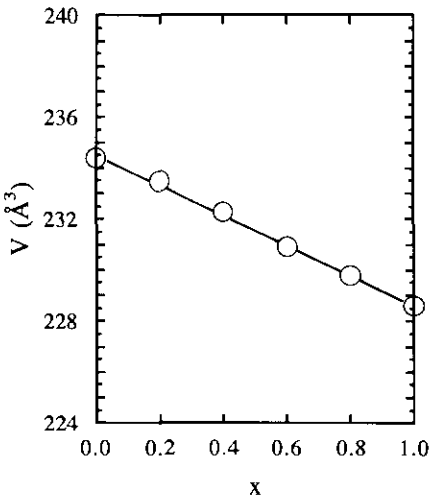

FIG. 3. Cell volume vs composition for the system $(La_{1-x}Nd_x)CrO_3$.

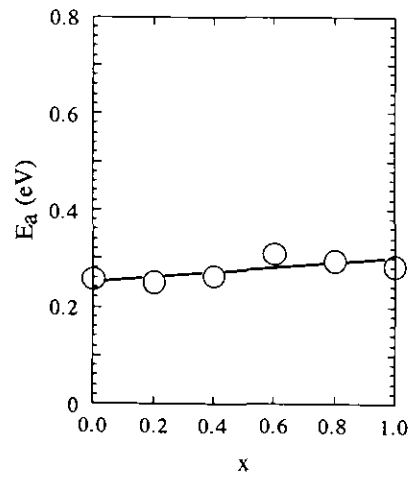

FIG. 5. Activation energy vs composition for the system $(La_{1-x}Nd_x)CrO_3$.

energy (E_a) from the linear portion of the log ρ–1000/T curves. E_a values for $LaCrO_3$ and $NdCrO_3$ are ca. 0.26 and ca. 0.28 eV, respectively. Figure 5 shows the relationship between E_a and the composition. E_a increases slightly with increasing x. Rao *et al.* reported that E_a for $LaCrO_3$ is ca. 0.22 eV (3). On the other hand, Ruiz *et al.* reported that E_a for $LaCrO_3$ is ca. 0.6 eV (10). The present E_a for $LaCrO_3$ is nearly equal to the value reported by Rao *et al.* (3).

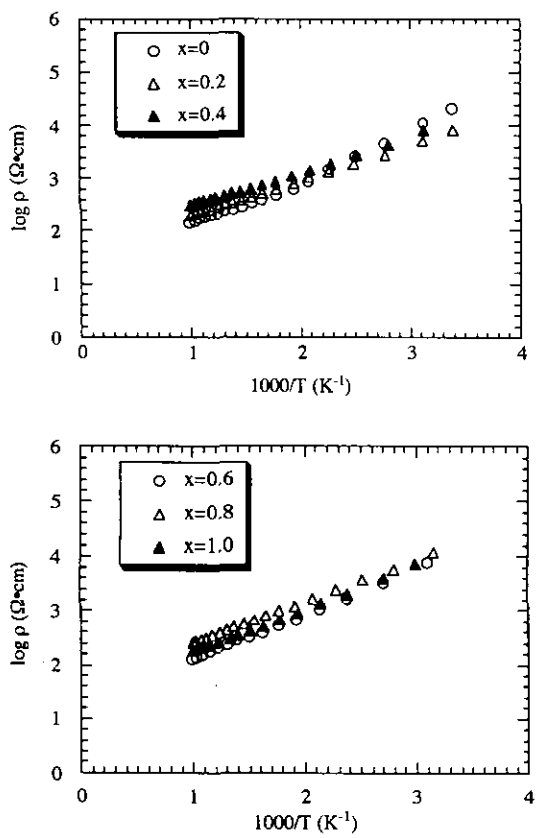

FIG. 4. Electrical resistivity vs 1000/T for the system $(La_{1-x}Nd_x)CrO_3$.

We carried out the structure refinement of $(La_{1-x}Nd_x)CrO_3$ by Rietveld analysis of X-ray powder diffraction data. $(La_{1-x}Nd_x)CrO_3$ has an orthorhombic $GdFeO_3$-type structure with the space group *Pnma* (11). In the present study, isotropic thermal parameters (B) for La, Nd, Cr, O(1), and O(2) ions were fixed at 0.3 Å^2 for all samples. Refined structural parameters and residuals R_{WP}, R_I, and R_F are listed in Table 1. R_{WP}, R_I, and R_F are the residuals for the weighted pattern, the integrated intensity, and the structure factor, respectively. Final R_I of all samples was less than 2.11%. The low R_I suggests that the structural model for $(La_{1-x}Nd_x)CrO_3$ is good.

In the orthorhombic $GdFeO_3$-type structure, the A-site cation (La and/or Nd ions) coordinates with 12 anions: 4 O(1) and 8 O(2) ions. The B-site cation (Cr ion) coordinates with 6 anions: 2 O(1) and 4 O(2) ions. We calculated the average (La, Nd)–O and Cr–O distance of $(La_{1-x}Nd_x)CrO_3$ from the refined structural parameters. Figure 6 shows the average (La, Nd)–O and Cr–O distances. The average (La, Nd)–O distance of $LaCrO_3$ is ca. 2.759 Å and decreases slightly to ca. 2.752 Å (x = 1.0) with increasing x. This decrease is due to the difference in ionic radius between the La^{3+} and Nd^{3+} ions. On the other hand, the average Cr–O distance of $LaCrO_3$ is ca. 1.971 Å, and increases slightly to ca. 1.978 Å (x = 1.0) with increasing x.

We calculated the angles for O–Cr–O and Cr–O–Cr of $(La_{1-x}Nd_x)CrO_3$ from the refined structural parameters. The average angles for O(1)–Cr–O(1) and

TABLE 1
Refined Structure Parameters for $(La_{1-x}Nd_x)CrO_3$

Atom	Position	x	y	z	B
$x = 0$, $a = 5.4786(1)$ Å, $b = 7.7573(1)$ Å, $c = 5.5146(1)$ Å, $R_{WP} = 10.48\%$, $R_I = 3.03\%$, and $R_F = 1.94\%$					
La	4(*c*)	0.020(1)	0.25	−0.004(1)	0.3
Cr	4(*b*)	0	0	0.5	0.3
O(1)	4(*c*)	0.493(5)	0.25	0.061(7)	0.3
O(2)	8(*d*)	0.273(6)	0.036(4)	−0.278(5)	0.3
$x = 0.2$, $a = 5.4768(2)$ Å, $b = 7.7510(2)$ Å, $c = 5.4996(2)$ Å, $R_{WP} = 9.58\%$, $R_I = 2.73\%$, and $R_F = 1.56\%$					
La, Nd	4(*c*)	0.024(1)	0.25	−0.005(1)	0.3
Cr	4(*b*)	0	0	0.5	0.3
O(1)	4(*c*)	0.490(5)	0.25	0.071(10)	0.3
O(2)	8(*d*)	0.278(6)	0.034(6)	−0.278(6)	0.3
$x = 0.4$, $a = 5.4762(2)$ Å, $b = 7.7387(2)$ Å, $c = 5.4807(2)$ Å, $R_{WP} = 10.60\%$, $R_I = 2.77\%$, and $R_F = 1.56\%$					
La, Nd	4(*c*)	0.029(1)	0.25	−0.006(1)	0.3
Cr	4(*b*)	0	0	0.5	0.3
O(1)	4(*c*)	0.486(6)	0.25	0.081(14)	0.3
O(2)	8(*d*)	0.282(9)	0.034(7)	−0.285(8)	0.3
$x = 0.6$, $a = 5.4736(3)$ Å, $b = 7.7367(4)$ Å, $c = 5.4521(3)$ Å, $R_{WP} = 14.15\%$, $R_I = 2.69\%$, and $R_F = 2.11\%$					
La, Nd	4(*c*)	0.033(1)	0.25	−0.006(1)	0.3
Cr	4(*b*)	0	0	0.5	0.3
O(1)	4(*c*)	0.491(7)	0.25	0.077(16)	0.3
O(2)	8(*d*)	0.290(9)	0.037(8)	−0.277(10)	0.3
$x = 0.8$, $a = 5.4754(2)$ Å, $b = 7.7154(4)$ Å, $c = 5.4388(3)$ Å, $R_{WP} = 12.26\%$, $R_I = 2.27\%$, and $R_F = 1.49\%$					
La, Nd	4(*c*)	0.037(1)	0.25	−0.008(1)	0.3
Cr	4(*b*)	0	0	0.5	0.3
O(1)	4(*c*)	0.487(7)	0.25	0.088(14)	0.3
O(2)	8(*d*)	0.290(7)	0.031(7)	−0.289(8)	0.3
$x = 1.0$, $a = 5.4829(1)$ Å, $b = 7.6919(1)$ Å, $c = 5.4203(1)$ Å, $R_{WP} = 10.03\%$, $R_I = 2.46\%$, and $R_F = 1.54\%$					
Nd	4(*c*)	0.041(1)	0.25	−0.009(1)	0.3
Cr	4(*b*)	0	0	0.5	0.3
O(1)	4(*c*)	0.484(5)	0.25	0.082(6)	0.3
O(2)	8(*d*)	0.293(4)	0.041(4)	−0.289(5)	0.3

O(1)–Cr–O(2) are 180° and 90°, respectively. The average angle for O(2)–Cr–O(2) is 90° or 180°. On the other hand, both the angles for Cr–O(1)–Cr and Cr–O(2)–Cr are less than 180° and decrease monotonically with increasing x, as shown in Fig. 7. Figure 8 shows a perspective view of the anionic chain in $(La_{1-x}Nd_x)CrO_3$. The CrO_6 octahedron connects at O(1) or O(2) of the other's CrO_6 octahedron. From the results of the Cr–O distance and the average angles for O–Cr–O, it is obvious that each CrO_6 octahedron has little distortion. The bending among the neighboring CrO_6 octahedra sharpens with increasing x.

Figure 9 shows the XPS spectra of the La3$d_{5/2}$, Nd3$d_{5/2}$, and Cr2$p_{3/2}$ levels of $(La_{1-x}Nd_x)CrO_3$. The binding energies of La3$d_{5/2}$, Nd3$d_{5/2}$, Cr2$p_{3/2}$, and O1$s_{1/2}$ are independent of the composition: 833.38 ± 0.18 eV for La3$d_{5/2}$, 981.17 ± 0.17 eV for Nd3$d_{5/2}$, 575.24 ± 0.11 eV for Cr2$p_{3/2}$, and 528.49 ± 0.14 eV for O1$s_{1/2}$. The full width at half-maximum of the Cr2$p_{3/2}$ level is ca. 2.44 eV and is independent of the composition. Taguchi and Shimada discussed the chemical bond of the orthorhombic perovskite-type $CaMnO_{3-\delta}$ from the binding energy difference (ΔBE) (12). ΔBE for Ca2p–O1s increases and ΔBE for Mn2p–O1s decreases with decreasing oxygen content. The increase in ΔBE indicates that the chemical bond becomes more ionic. In the present study, ΔBE for La3$d_{5/2}$–O1$s_{1/2}$, Nd3$d_{5/2}$–O1$s_{1/2}$, and Cr2$p_{3/2}$–O1$s_{1/2}$ are independent of the composition: 304.92 ± 0.15 eV for La3$d_{5/2}$–O1$s_{1/2}$, 452.67 ± 0.18 eV for Nd3$d_{5/2}$–O1$s_{1/2}$, and 46.75 ± 0.09 eV for Cr2$p_{3/2}$–O1$s_{1/2}$. These results

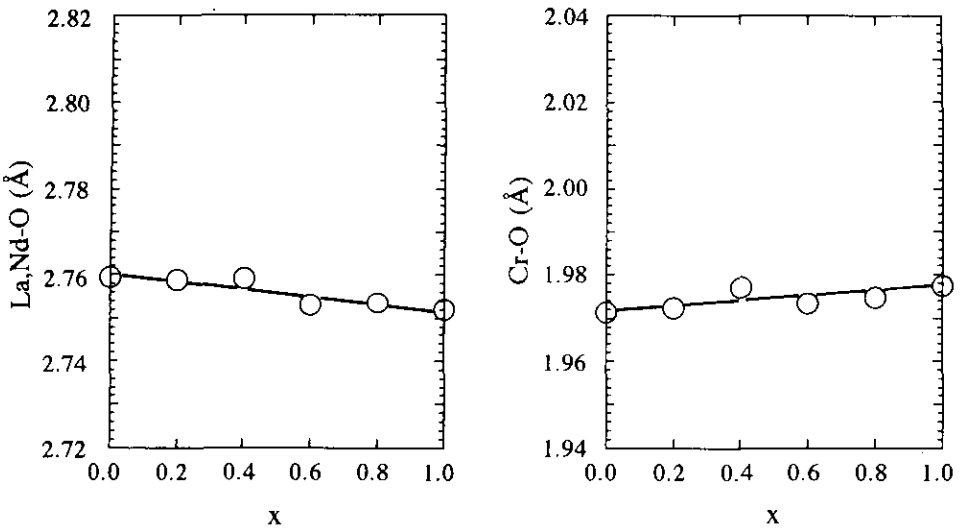

FIG. 6. Average (La, Nd)–O and Cr–O distances vs composition for the system $(La_{1-x}Nd_x)CrO_3$.

suggest that the chemical bond for La–O, Nd–O, or Cr–O is not affected by the composition.

From the results of the Rietveld analysis and XPS measurements for $(La_{1-x}Nd_x)CrO_3$, it is obvious that the Cr–O distance of the CrO_6 octahedron increases slightly with increasing x; however, each CrO_6 octahedron has little distortion. The decrease of the angles for Cr–O(1)–Cr or Cr–O(2)–Cr is caused by the linear decrease of the cell volume. The electronegativity values of La and Nd are 1.1 and 1.2, respectively (13). From these results of the electronegativity and Cr–O distance, it is believed that the chemical bond for Cr–O is not affected by the composition.

According to the one-electron energy diagram for La CrO_3 (4), three $3d$-electrons of the Cr^{3+} ion are all localized and the Fermi level lies between the filled t_{2g}* levels and the narrow σ* band orbitals. From the electronic spectra, the energy of excitation (10 Dq) is experimentally found to be ca. 2.0 eV (10). The activation energy (E_a) is half of 10 Dq; that is, ca. 1.0 eV. However, the measured E_a is smaller than 1.0 eV. Therefore, Rao *et al.* proposed that the Cr^{4+} ions present as a result of impurities or native defects give rise to p-type extrinsic conduction in $LaCrO_3$ (3). Due to the slight increase in the Cr–O distance and the decrease of the angle for Cr–O(1)–Cr or Cr–O(2)–Cr, the overlap between the chromium t_{2g} and oxygen p_π orbitals decreases slightly with increasing x. Although we could

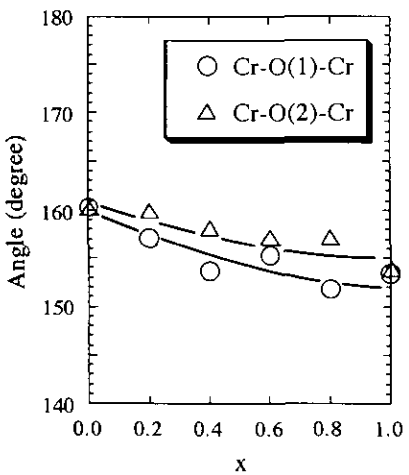

FIG. 7. Angles for Cr–O(1)–Cr and Cr–O(2)–Cr vs composition for the system $(La_{1-x}Nd_x)CrO_3$.

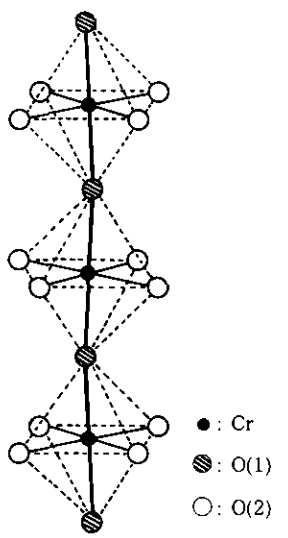

FIG. 8. Perspective view of the anion chain in $(La_{1-x}Nd_x)CrO_3$.

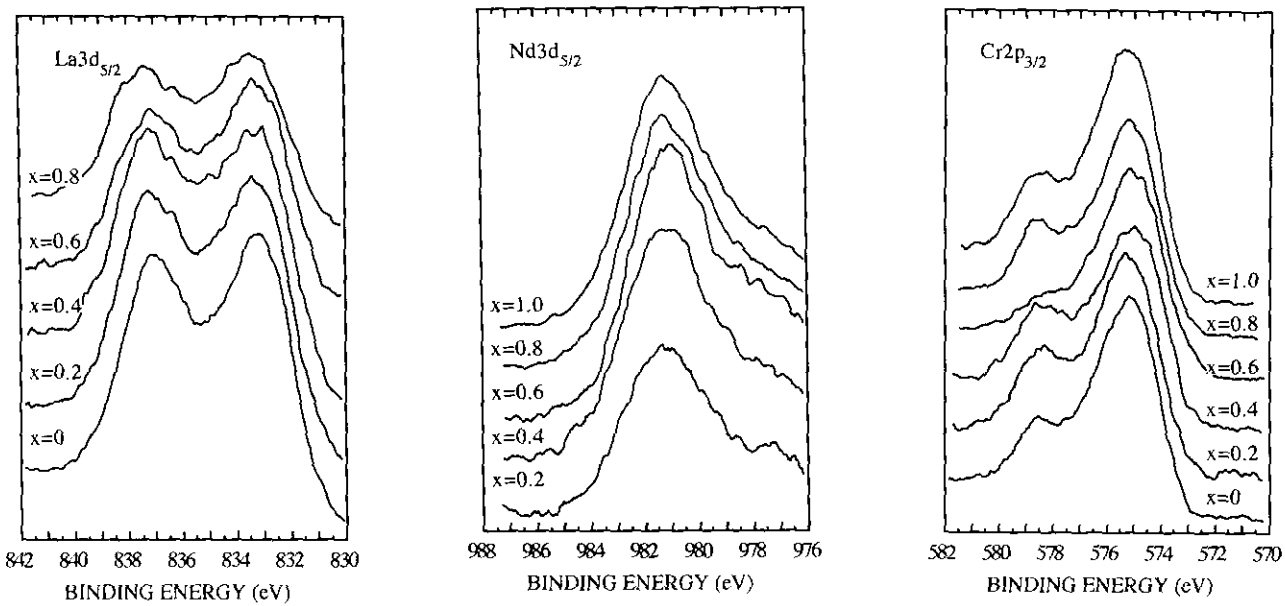

FIG. 9. XPS spectra of the La3$d_{5/2}$, Nd3$d_{5/2}$, and Cr2$p_{3/2}$ levels for the system $(La_{1-x}Nd_x)CrO_3$.

not find significant change in the electrical resistivity as shown in Fig. 4, E_a as shown in Fig. 5 is affected by the composition.

CONCLUSION

Although the cell volume of $(La_{1-x}Nd_x)CrO_3$ decreases linearly with increasing x, Rietveld analysis and XPS measurements indicate that the decrease of the angles for Cr–O(1)–Cr or Cr–O(2)–Cr is due to the linear decrease in the cell volume. The chemical bond for Cr–O is not affected by the composition. $(La_{1-x}Nd_x)CrO_3$ are p-type semiconductors with an activation energy of ca. 0.26 to 0.28 eV. Although significant compositional dependence in the electrical resistivities was not found, the activation energy increases slightly with the composition. This increase is caused by the slight decrease of the overlap between the chromium t_{2g} and oxygen p_π orbitals.

REFERENCES

1. T. Arakawa, S. Tsuchi-Ya, and J. Shiokawa, *Mater. Res. Bull.* **16,** 97 (1981).
2. J. B. Goodenough and J. M. Longo, "Landolt-Bornstein, Group III, Vol. 4, Magnetic and Other Properties of Oxides and Related Compounds," p. 228. Springer–Verlag, New York, 1970.
3. G. V. S. Rao, B. M. Wanklyn, and C. N. R. Rao, *J. Phys. Chem. Solids* **32,** 345 (1971).
4. J. B. Goodenough, *J. Appl. Phys.* **37,** 1415 (1966).
5. J. B. Macchesney, R. C. Sherwood, and J. F. Potter, *J. Chem. Phys.* **43,** 1907 (1965).
6. B. D. Cullity, "Elements of X-ray Diffraction," p. 506. Addison–Wesley, Reading, MA, 1978.
7. F. Izumi, *Nippon Kesho Gakkaishi* **27,** 23 (1985). [in Japanese]
8. R. D. Shannon and C. T. Prewitt, *Acta Crystallogr., Sect. B* **25,** 925 (1969).
9. R. D. Shannon, *Acta Crystallogr. Sect., A* **32,** 751 (1976).
10. J. S. Ruiz, A. M. Anthony, and M. Foex, *Compt. Rend. B* **264,** 1271 (1967).
11. K. R. Poeppelmeier, M. E. Leonowicz, J. C. Scanlon, and W. B. Yelon, *J. Solid State Chem.* **45,** 71 (1982).
12. H. Taguchi and M. Shimada, *Phys. Status Solidi B* **131,** K59 (1985).
13. W. Gordy and W. J. Oriville Thomas, *J. Chem. Phys.* **24,** 439 (1956).